BEAM DYNAMICS ACTIVITIES AT SLS

M. Böge, J. Chrin, G. Ingold, T. Schilcher, T. Schmidt, A. Streun

While SLS is running well in user operation, further development of the machines continues. In 2004 beam dynamics activities focussed on the dynamic orbit stabilization and on the compensation of orbit distortions from undulator gap variations. The storage ring was tuned for FEMTO operation by breaking its symmetry and moving to a new working point, and some measurements of lifetime and acceptance were done. The performance of the booster synchrotron was improved by retuning its ramping curve.

FAST ORBIT FEEDBACK (FOFB): OPERATIONAL EXPERIENCE AND PERFORMANCE

The FOFB has been running routinely in user operation since November 2003. The overall reliability of hardware and software has been the main focus during the first phase of operation. Therefore, the FOFB has been operated at moderate PID loop gains and DBPM filter settings, providing a regulation bandwidth of ≈ 60 Hz [1] during the first couple of months. In order to avoid beam loss due to possible malfunctioning FOFB components, a low level software security package has been implemented which monitors the parameters of the FOFB and the performance of its subsystems. When exceeding predefined corrector magnets dead bands, the FOFB is automatically stopped and a corresponding alarm is displayed to the operator, who can thus decide to call an expert or to continue with FOFB operation. So far, the FOFB has shown an overall availability of > 95 %. Although some automatic interruptions of the FOFB have been caused by malfunctioning of Digital Beam Position Monitoring (DBPM) electronics and corrector magnet power supplies, a growing number of FOFB interruptions are caused by users who perform beamline commissioning during regular user shifts.

Although the overall loop delay, which has been measured to be approximately 1.6 ms, could not be reduced by a DBPM firmware upgrade, the synchronization of all DBPM electronics allowed the use of a more stringent set of PID parameters, which finally led to the operation of the FOFB close to its design parameters [2]: frequencies up to nearly 100 Hz in both transverse planes are attenuated by the FOFB in its present mode of operation. Fig. 1 shows the measured FOFB closed loop transfer function for both transverse planes. Orbit perturbations up to 100 Hz are effectively damped, while noise sources between 100 Hz and 300 Hz are moderately excited.

Tab. 1 summarizes the improvements of beam stability at the SLS with the FOFB running compared to the situation without feedback. The values still contain the noise contribution of the DBPM system, which has been measured to be < 0.13 μm within the FOFB bandwidth. Orbit distortions caused by Insertion Device (ID) gap changes, which lead to severe orbit perturbations when the FOFB is **not** active, are **not** included. The temporal RMS values are integrated over the active range of the FOFB (up to 100 Hz) and up to 150 Hz, where significant noise contributions

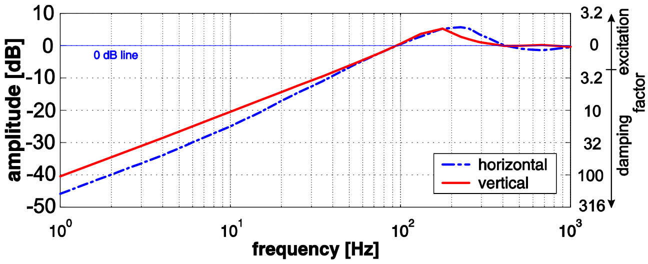

Fig. 1: Measurement of FOFB closed loop transfer functions in both transverse planes. Effective attenuation of orbit perturbations has been achieved close to the FOFB design goal of 100 Hz.

could still be observed. The RMS values at a location s in the storage ring are obtained from the table by multiplication with $\sqrt{\beta_{x/y}(s)}$.

At the source points of the low gap IDs with $\beta_y \approx 0.9$ m this translates to vertical RMS values of $\sigma_y = 0.25$ μm integrated up to 100 Hz.

Apart from the improved integrated beam stability up to 100 Hz, the FOFB allows autonomous and independent changes of ID gaps as well as beamline optimization by the users. Tests with rapidly moving ID gaps and correctors have shown that the resulting orbit kicks are invisible to all other users when the FOFB is active. Since beam position information in the FOFB architecture is only distributed locally [2] and dispersion fits in each sector are based on 18 out of 72 beam position readings at a rate of 4 kHz, the low level part of the feedback corrects off-energy trajectories only on a micron level. Resulting slow drifts of the dispersion orbit and horizontal mean corrector kicks are avoided by a high-level beam dynamics application, which adds suitable offsets to horizontal corrector currents and RF frequency every 20-30 minutes [3].

	horizontal		vertical	
FOFB	off	on	off	on
1-100 Hz	0.83 μm	0.38 μm	0.40 μm	0.27 μm
100-150 Hz	0.08 μm	0.17 μm	0.06 μm	0.11 μm
1-150 Hz	0.83 μm	0.41 μm	0.41 μm	0.29 μm

Table 1: Integrated beam position temporal RMS values with FOFB off and on at the tune BPM normalized to the beta function $\beta_{x/y} \approx 12/17$ m for fixed ID gaps.

A slow high level feedback application based on the X-Ray BPM (XBPM) readings provides sub-μm RMS beam stability at the first optical elements of the beamlines [4]. The slow feedback applies an asymmetric bump by changing the reference orbit of the FOFB thus implementing a cascaded feedback scheme.

A systematic oscillation with a period of ≈ 45 min showed up on the reference orbit changes. This oscillation was originally suspected to be a temperature effect in the four-channel DBPM electronics (Fig. 2). However, measurements of the DBPM rack temperatures only showed a correlation with other systematic long-term drifts. Finally the time constant of the 45 min oscillation could be correlated with the injection clock cycle, which constantly sweeps over the buckets to be filled in the storage ring during "top-up" operation. A corresponding bunch pattern dependency in the RF front-end of the DBPM electronics has been demonstrated to be the reason for the orbit oscillations. A bunch pattern feedback in the storage ring has been implemented to eliminate this effect (lower plot in Fig. 2) [5]. The remaining drift is mainly due to air temperature variations at the location of the BPM electronics.

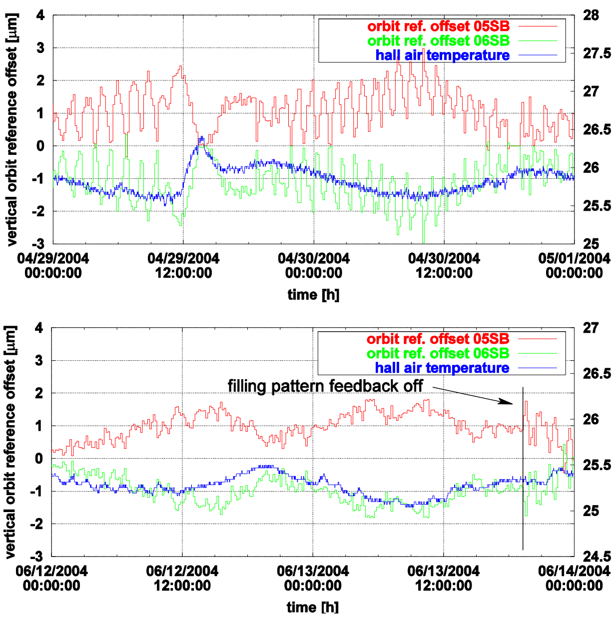

Fig. 2: FOFB reference orbit changes of the two RF BPMs (05SB, 06SB) adjacent to the ID. An asymmetric bump is applied by a high level slow feedback in order to keep the XBPM reading constant. With the filling pattern feedback a 40-50 minute oscillation (upper plot) due to a filling pattern dependence of the BPM system could be eliminated (lower plot). The remaining drift is mainly due to air temperature variations at the location of the BPM electronics.

INSERTION DEVICES FEED FORWARD (IDFF)

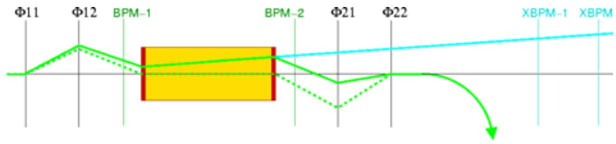

Fig. 3: The ID Feed Forward correction scheme.

Undulators and wigglers show small variations of the field integral (i.e. net deflection angle, which should be zero) as a function of gap and other parameters, causing orbit distortions during changes of their status. The FOFB system is able to decouple different beamlines, i.e. an orbit distortion created by moving one ID is not seen in the other straight sections. However, since the orbit distortion is a predictable and unique function of the gap and, in some cases, can also be quite large, it is advantageous to take steps to cancel the predicted distortion in advance, by means of a hardwired ID feed forward (IDFF) table, in order to lighten the burden of the FOFB. Data acquisition for compilation of the forward tables also includes the dedicated local BPMs, positioned immediately before and after each insertion device, as well as the XBPMs in the beamline front end, in order to keep the photon beam emitted by the ID at its predefined position. The procedure as sketched in Fig. 3 is performed in two steps:

1. Assuming that the orbit distortion is created by kicks at entry and exit of the ID (which is the most likely assumption due to the typical edge field behaviour), these kicks are extracted by analyzing the response of all 72 storage ring BPMs to the gap variation. The local corrector deflection angles (Φ_{ij}) at the ID are set to compensate for the edge kicks (basically this is a 2-corrector orbit correction) as indicated by the solid line in the figure above.
2. Reading local BPMs and XBPMs the photon beam position is fitted using weighting factors adapted to the gap-dependant significance of the different monitors (e.g. the XBPM provides no information at large gap). The local correctors are incremented by the appropriate currents to keep the photon beam in place (dotted line in above figure).

This method, already described in [6], has now reached maturity and is routinely applied to all in-vacuum undulators at SLS. For the elliptical undulators only the local BPMs are used to date. Inclusion of the XBPMs requires further refinement, since the photon beam shape varies with the polarization state of the ID.

As an example, Fig. 4 shows the horizontal and vertical photon beam position in beamline 6S as a function of undulator gap for two cases: (i) with only the FOFB running and no IDFF applied (curved solid lines, split into two lines due to small hysteresis effects when opening or closing the gap), and (ii) with

FOFB running **and** the IDFF applied (solid, almost flat lines). Best results are obtained if the XBPMs are also included in the FOFB (star/cross-dotted lines): the residual photon beam variation is of the order of 1 μm.

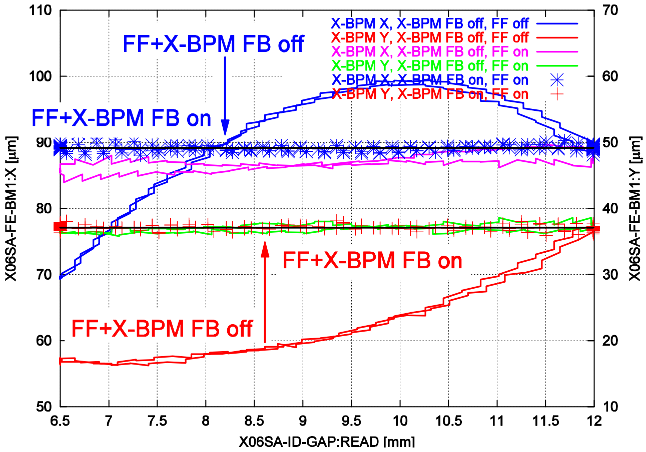

Fig. 4: Stabilization of photon beam during undulator gap variation by application of feed forward tables and FOFB with XBPM integration.

FEMTO OPTICS

The FEMTO beamline [7] for generation of sub-picosecond X-Ray pulses will become operational in 2005. The storage ring has been modified by installation of the U19 radiator undulator for the μXAS beamline, and a central triplet to obtain a vertical focus in U19 and the required optics for extraction of the FEMTO satellites [8]. This modification breaks the 3-fold symmetry of the ring. However, the additional betatron phase advances due to the modification amount to exactly 180° vertical and 0° horizontal, furthermore all changes of optical functions are confined to a region without sextupoles. For this particular case, the sextupoles cannot “see” the symmetry breaking and thus the dynamic acceptance of the storage ring should not be affected. In fact, after shifting the working point Q_x / Q_y from 20.42 / 8.**19** to 20.42 / 8.**69** by powering the triplet and the adjacent quadrupoles, no deterioration of injection efficiency or lifetime was observed. Fig. 5 shows the beta functions in straight section 5L for the previous (dotted) and new (solid) optics.

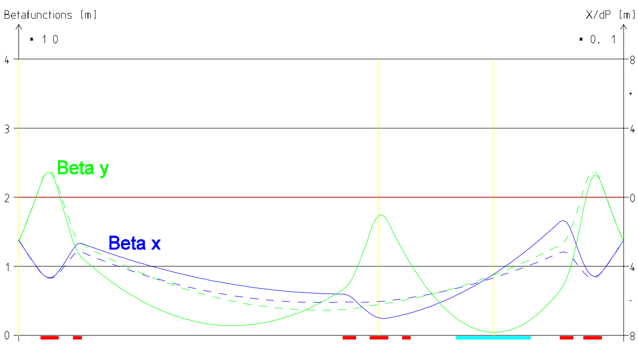

Fig. 5: Betafunctions in 5L for FEMTO (solid) and previous (dotted) optics.

LIFETIME AND ACCEPTANCE MEASUREMENTS

Elastic scattering of beam electrons on residual gas nuclei and Touschek scattering between two beam electrons are the main mechanisms for particle losses in the SLS storage ring. The beam lifetime from elastic scattering alone is proportional to the available transverse acceptance and inversely proportional to the residual gas pressure. The acceptance is fully dominated by the vertical acceptance because the vacuum chamber height is small compared to its width. The acceptance can be varied by slowly moving a scraper into the beam. Several such measurements have been done; an example is shown in Fig. 6. As the scraper closes the lifetime is not affected as long as the scraper remains within a “shadow area”, defined by the storage ring acceptance limitation.

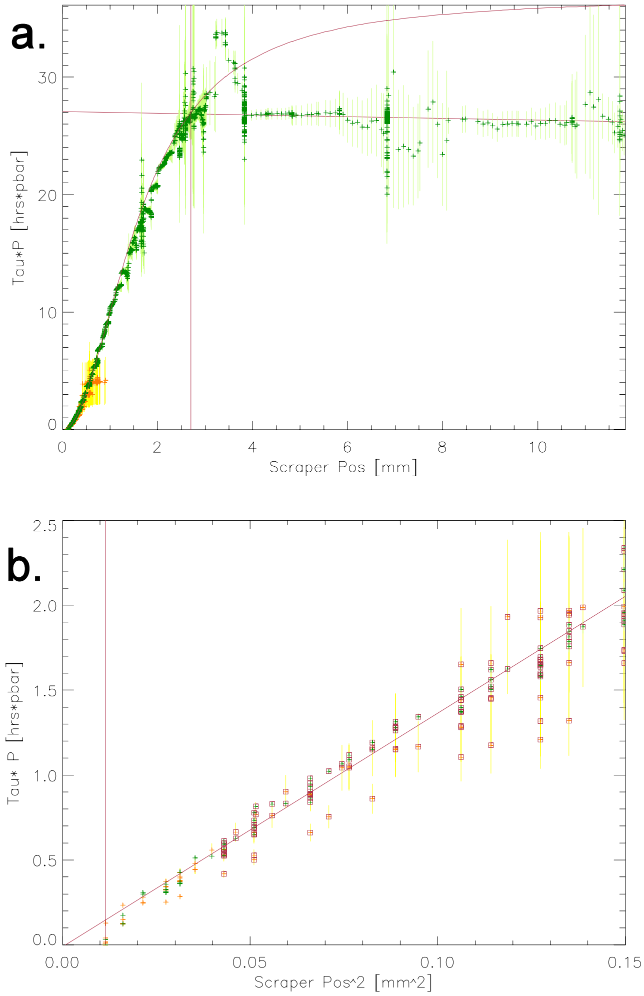

Fig. 6: A typical scraper measurement for the determination of the storage ring transverse acceptance:

- **a.** Lifetime (normalized to residual gas pressure) versus scraper position. The vertical line defines the storage ring acceptance.
- **b.** Magnified view of lifetime versus the square of the scraper position, which is proportional to the acceptance determined by the scraper. The vertical line defines the beam size, i.e., where the scraper enters the Gaussian tails.

Where the scraper defines the acceptance, lifetime is proportional to the square of its position (parabolic shape in Fig. 6.a, left region; straight line in Fig. 6.b). The onset of the scraper dominance defines the storage ring acceptance (vertical line in Fig. 6.a). Finally, the beam is destroyed when the scraper touches its Gaussian tails; in this regime, beam lifetime is very low and deviates from the square law. The onset (vertical line in Fig. 6.b) allows the beam size to be estimated. Finally other lifetime contributions (mainly Touschek scattering) may be estimated to determine what the lifetime would be without any acceptance limitation (curve in Fig. 6.a).

Detailed lifetime studies had been done earlier [9], but due to continuous upgrades and modifications of SLS, these scraper measurements are repeated routinely. All measurements in 2004 are consistent with a vertical acceptance of 0.9 (±0.1) mm mrad and an emittance ratio (vertical to horizontal) of about 1.0 (±0.3) %. The absolute lifetime values are compatible with a residual gas composition of 20 % CO / 80 % H_2.

The measured acceptance is about three times smaller than expected, indicating the existence of an obstacle somewhere in the storage ring, which hopefully will be identified in 2005.

BOOSTER RAMP OPTIMIZATION

The SLS booster synchrotron accelerates electrons from 100 MeV to 2.4 GeV within 146 ms following a sinusoidal ramping curve for all magnets. Due to remanences, hysteresis and eddy currents, the magnetic fields do not precisely follow the ideal ramp. Consequently, beam parameters such as tunes and chromaticities vary during the ramp leading to partial beam loss; e.g. when a betatron resonance is crossed. Fortunately, all power supplies have programmable waveforms, which may be set to "equalize" the magnet strengths interactively in order to keep tunes and chromaticities constant [10].

Some experiments with the linac and booster are performed parasitically to top-up operation of the storage ring. This is possible by running the injection chain continuously and extracting beam from the booster only when required to maintain the desired stored current. Between these extractions the beam is decelerated again in the booster and finally lost at low energy. By careful equalization of the ramp the final energy after deceleration was reduced from approx. 300 MeV to 70 MeV in 2004, in order to minimize the radiation within the ring tunnel.

Since commissioning, the booster is operating at a working point Q_x / Q_y near 12.4 / 8.4 providing good performance but located near a main coupling resonance. Consequently, the beam is fully coupled, and the vertical emittance at extraction is as large as the horizontal one. The vertical emittance was measured in the BR transfer line by observing the beam spot on an OTR screen and variation of an upstream quadrupole, and found to be 10.5 nm rad, which is as large as the horizontal one (10.0 nm rad). A new working point at 12.26 / 8.44, far from the resonance was established and equalized successfully, and in fact the vertical emittance dropped to 2 nm rad. However, an improvement of injection efficiency into the storage ring, as was expected considering the rather narrow vertical ring acceptance, has not yet been achieved.

OUTLOOK

For SLS beam dynamics, 2004 was a year of continuous improvements rather than dramatic advancements. This will be different next year facing FEMTO and superbend commissioning. Pinger magnets for single turn horizontal and vertical beam excitation will be installed and will provide detailed insight into the dynamics of the stored beam.

REFERENCES

[1] T. Schilcher et al., *Commissioning and Operation of the SLS Fast Orbit Feedback*, PSI Scientific Report 2003, VI.

[2] M. Böge, *Transverse Stabilization of the SLS Beam*, PSI Scientific Report 1998, VII.

[3] M. Böge, *Slow and Fast Orbit Feedback*, PSI Scientific Report 2003, VI.

[4] J. Krempaský, T. Schilcher, V. Schlott, *Insertion Device Photon Beam Studies with X-Ray Monitors*, PSI Scientific Report 2003, VI.

[5] B. Kalantari, V. Schlott, T. Korhonen, *Bunch Pattern Control in Top-up Mode at the SLS*, PSI Scientific Report 2004.

[6] T. Schmidt, J. Chrin, A. Streun, D. Zimoch, *Feed Forward Corrections for Insertion Devices at the SLS,* PSI Scientific Report 2003, VI.

[7] G. Ingold et al., *Conceptual Design: Sub-picosecond hard X-Ray source*, PSI Scientific Report 2001, VII.

[8] A. Streun, *SLS-FEMTO: Chicane layout, performance and side effects*, PSI Internal Report SLS-TME-TA-2003-0223.

[9] A. Streun, *Beam lifetime in the SLS storage ring,* PSI Internal Report SLS-TME-TA-2001-0190.

[10] M. Muñoz, *Experience with the SLS booster*, Proceedings EPAC'02, Paris June 2002.